Alzheimer Disease: Quantitative Structural Neuroimaging for Detection and Prediction of Clinical and Structural Changes in Mild Cognitive Impairment[1]

Linda K. McEvoy, PhD
Christine Fennema-Notestine, PhD
J. Cooper Roddey, PhD
Donald J. Hagler, Jr, PhD
Dominic Holland, PhD
David S. Karow, MD
Christopher J. Pung, BA
James B. Brewer, MD, PhD
Anders M. Dale, PhD
For the Alzheimer's Disease Neuroimaging Initiative

Purpose: To use structural magnetic resonance (MR) images to identify a pattern of regional atrophy characteristic of mild Alzheimer disease (AD) and to investigate whether presence of this pattern prospectively can aid prediction of 1-year clinical decline and increased structural loss in mild cognitive impairment (MCI).

Materials and Methods: The study was conducted with institutional review board approval and compliance with HIPAA regulations. Written informed consent was obtained from each participant. High-throughput volumetric segmentation and cortical surface reconstruction methods were applied to MR images from 84 subjects with mild AD, 175 with MCI, and 139 healthy control (HC) subjects. Stepwise linear discriminant analysis was used to identify regions that best can aid discrimination of HC subjects from subjects with AD. A classifier trained on data from HC subjects and those with AD was applied to data from subjects with MCI to determine whether presence of phenotypic AD atrophy at baseline was predictive of clinical decline and structural loss.

Results: Atrophy in mesial and lateral temporal, isthmus cingulate, and orbitofrontal areas aided discrimination of HC subjects from subjects with AD, with fully cross-validated sensitivity of 83% and specificity of 93%. Subjects with MCI who had phenotypic AD atrophy showed significantly greater 1-year clinical decline and structural loss than those who did not and were more likely to have progression to probable AD (annual progression rate of 29% for subjects with MCI who had AD atrophy vs 8% for those who did not).

Conclusion: Semiautomated, individually specific quantitative MR imaging methods can be used to identify a pattern of regional atrophy in MCI that is predictive of clinical decline. Such information may aid in prediction of patient prognosis and increase the efficiency of clinical trials.

[1] From the Departments of Radiology (L.K.M., C.F., D.J.H., D.S.K., C.J.P., J.B.B., A.M.D.), Neuroscience (J.C.R., D.H., J.B.B., A.M.D.), and Psychiatry (C.F.), University of California, San Diego, 9500 Gilman Dr, La Jolla, CA 92093-0841. Received June 4, 2008; revision requested July 16; revision received September 10; accepted September 26; final version accepted October 13. **Address correspondence to** L.K.M. (e-mail: *lkmcevoy@ucsd.edu*).

Data used in the preparation of this article were obtained from the Alzheimer's Disease Neuroimaging Initiative (ADNI) database (*http://www.loni.ucla.edu/ADNI*). As such, the investigators within the ADNI contributed to the design and implementation of ADNI and/or provided data but did not participate in analysis or writing of this report. The complete listing of ADNI investigators is available at *http://www.loni.ucla.edu/ADNI/Data/ADNI_Authorship_List.pdf*.

Mild cognitive impairment (MCI) is associated with an increased risk of progression to a diagnosis of probable Alzheimer disease (AD) (1–4). Rates of progression vary; some individuals with MCI deteriorate rapidly, others remain stable for many years, and some revert to normal cognitive status. Improved ability to predict risk of imminent decline in patients with MCI could aid in the efficiency of large-scale clinical trials and will become increasingly important for individual patient risk stratification as aggressive new treatments are developed.

Structural neuroimaging measures are sensitive to the degeneration that occurs in mild AD and MCI (5) and may be predictive of disease progression (6–16). However, most prior studies have been limited by small samples or use of data from one site. Researchers in many studies have used manual tracing methods, which are not practical for clinical use or use in large-scale clinical trials. Others have used automated approaches that are based on statistical parametric mapping, such as voxel-based morphometry, that can efficiently aid assessment of disease-related structural differences across the brain (17) but are intended for group comparisons and not individual patient assessment (18). Furthermore, these methods provide an indirect measure of structural differences between groups that does not readily translate into quantitative change of specific anatomic structures involved in the disease.

In contrast, semiautomated methods that are based on the publicly available brain MR imaging software package (FreeSurfer; Athinoula A. Martinos Center for Biomedical Imaging, Massachusetts General Hospital, Boston, Mass) produce complete voxel-based segmentation, as well as cortical surface reconstruction and parcellation of each individual's brain (19–25), with high reproducibility and accuracy comparable to that of manual labeling (21,23,26,27). These methods can be applied to individual subject data and are sensitive to the structural changes that occur in normal aging (28), MCI, and AD (23,29).

Researchers in prior studies have found that atrophy of mesial temporal structures, such as the hippocampus and entorhinal cortex, is predictive of progression to AD (6,30–33), particularly when rate of loss over time is examined (11,34,35). However, mesial temporal lobe atrophy is not specific to AD (36,37). By examining atrophy in widespread cortical areas, we hoped to identify a pattern of regional atrophy that is specific to AD and is useful for predicting disease progression. We focused on determining the predictive capability of single-time magnetic resonance (MR) imaging measures, rather than change over time, because the capability to identify subjects at risk of imminent decline from a baseline MR image would be of greater practical value for use as an enrichment strategy in clinical trials than reliance on information from images repeatedly obtained over a 6-month or 1-year interval. Thus, the purpose of our study was to use structural MR images to identify a pattern of regional atrophy characteristic of mild AD and to investigate whether the presence of this pattern can help prospectively predict 1-year clinical decline and increased structural loss in MCI.

Advances in Knowledge

- Semiautomated quantitative MR imaging analytic techniques that are suitable for use in large-scale clinical trials can be used to discriminate between subjects with mild Alzheimer disease (AD) and healthy control subjects, with high sensitivity (83%) and specificity (93%).
- In patients with amnestic mild cognitive impairment (MCI), those who have a pattern of regional atrophy characteristic of AD at baseline show greater clinical decline and structural loss over a 1-year period than those who lack the pattern of atrophy characteristic of AD.

Implication for Patient Care

- Identification of a pattern of regional atrophy that is characteristic of AD in patients with amnestic MCI could be used to increase the efficiency of large-scale clinical treatment trials and has the potential to aid in prediction of prognosis for individual patients.

Materials and Methods

Anders M. Dale, PhD, is a founder of and holds equity in CorTechs Labs, La Jolla, Calif, and also serves on the Scientific Advisory Board. The terms of this arrangement have been reviewed and approved by the University of California, San Diego, Calif, in accordance with its policies about conflict of interest. The authors had control of the data and the information submitted for publication.

Alzheimer's Disease Neuroimaging Initiative

Data used in this article were obtained from the home page of the Alzheimer's

Published online before print
10.1148/radiol.2511080924

Radiology 2009; 251:195–205

Abbreviations:
AD = Alzheimer disease
ADNI = Alzheimer's Disease Neuroimaging Initiative
CDR = Clinical Dementia Rating
HC = healthy control
LDA = linear discriminant analysis
MCI = mild cognitive impairment
MMSE = Mini-Mental State Examination
ROI = region of interest

Author contributions:
Guarantors of integrity of entire study, L.K.M., C.F., J.B.B., A.M.D.; study concepts/study design or data acquisition or data analysis/interpretation, all authors; manuscript drafting or manuscript revision for important intellectual content, all authors; manuscript final version approval, all authors; literature research, L.K.M., J.C.R., D.S.K., J.B.B., A.M.D.; experimental studies, C.F., J.B.B.; statistical analysis, L.K.M., C.F., J.C.R., D.J.H., A.M.D.; and manuscript editing, L.K.M., C.F., J.C.R., D.J.H., C.J.P., J.B.B., A.M.D.

Funding:
This research was supported by the National Center for Research Resources (grant no. U24RR021382), National Institute on Aging (grant nos. R01AG22381, K01AG029218-01A1), and National Institutes of Health (grant no. U01 AG024904).

See Materials and Methods for pertinent disclosures.

Disease Neuroimaging Initiative (ADNI) database at the LONI Web site (*http://www.loni.ucla.edu/ADNI*) published in 2007 (38). The ADNI was launched in 2003 by the National Institute on Aging, the National Institute of Biomedical Imaging and Bioengineering, the Food and Drug Administration, private pharmaceutical companies, and nonprofit organizations as a $60-million 5-year public-private partnership. The primary goal of the ADNI has been to test whether serial MR imaging, positron emission tomography, other biological markers, and clinical and neuropsychologic assessment can be combined to measure the progression of MCI and early AD. Determination of sensitive and specific markers of very early AD progression is intended to aid researchers and clinicians to develop new treatments and monitor their effectiveness, as well as lessen the time and cost of clinical trials.

The principal investigator of this initiative is Michael W. Weiner, MD, VA Medical Center and University of California, San Francisco, San Francisco, Calif. The ADNI is the result of efforts of many coinvestigators from a broad range of academic institutions and private corporations, and subjects have been recruited from more than 50 sites across the United States and Canada. The ADNI has recruited 229 cognitively healthy older individuals to be followed up for 3 years, 398 people with amnestic MCI to be followed up for 3 years, and 192 people with early AD to be followed up for 2 years. Up-to-date information is available from the home page of the ADNI-Info Web site at *http://www.adni-info.org* for 2009.

The prospective research protocol was approved by each local institutional review board, and written informed consent was obtained from each participant. The study is conducted in compliance with Health Insurance Portability and Accountability Act regulations.

Participants

The ADNI general eligibility criteria are described in the ADNI Protocol Summary page of the ADNI-Info Web site at *http://www.adni-info.org/index.php?option=com_content&task=view&id=9&Itemid=43* for 2009. Briefly, subjects are 55–90 years old, are not depressed, have a modified Hachinski score of 4 or less, and have a study partner able to provide an independent evaluation of functioning. Healthy control (HC) subjects have a Clinical Dementia Rating (CDR) (39) of 0. Subjects with MCI have a subjective memory complaint, objective memory loss measured by using education-adjusted scores on the Logical Memory II (Delayed Recall) subscale of the Wechsler Memory Scale, a CDR of 0.5, preserved activities of daily living, and an absence of dementia. Subjects with AD have a CDR of 0.5 or 1.0 and meet National Institute of Neurological Disorders and Stroke and Alzheimer's Disease and Related Disorders Association criteria for probable AD (40). Full details are available from the ADNI Protocol page of the ADNI-Info Web site at *http://www.adni-info.org/images/stories/Documentation/adni_protocol_9_19_08.pdf* published on September 19, 2008.

Raw baseline MR imaging data were downloaded as they became available, up until March 7, 2007, from the LONI Image Data Archive, ADNI Data database, published by LONI (Los Angeles, Calif) in 2007. In this study, we used baseline data collected prior to March 7, 2007, and included data from 139 HC subjects, 175 subjects with MCI, and 84 subjects with AD. Group clinical and demographic data are presented in Table 1. Clinical follow-up data were available on 160 subjects with MCI.

Procedures

Image acquisition and analytic methods were developed within the Morphometry Biomedical Informatics Research Network sponsored by the National Institutes of Health and the National Center for Research Resources and the ADNI (41–44). Data were collected from studies with a variety of 1.5-T MR imaging units. Much effort was expended in the ADNI develop-

Table 1

Group Demographics

Group	HC Subjects ($n = 139$)	Subjects with MCI ($n = 175$)	Subjects with Mild AD ($n = 84$)	Statistical Comparison
Sex				
Male*	77 (55)	123 (70)	51 (61)	$\chi^2 = 7.63$, $df = 2$, $P = .022$
Female*	62 (45)	52 (30)	33 (39)	. . .
Age (y)†	75.7 ± 5.01 (62–90)	74.7 ± 7.39 (55–89)	76.0 ± 7.61 (57–88)	$F = 0.82$; $df = 2, 395$; $P = .442$
Male†	75.5 ± 5.30 (63–88)	75.1 ± 7.17 (55–89)	75.6 ± 7.34 (57–88)	. . .
Female†	75.9 ± 4.66 (62–90)	73.8 ± 7.91 (55–86)	73.5 ± 7.81 (57–88)	. . .
Education (y)†	16.0 ± 3.01 (6–20)	16.0 ± 2.76 (8–20)	14.8 ± 3.05 (4–20)	$F = 5.70$; $df = 2, 395$; $P = .004$
MMSE score†	29.1 ± 1.01 (25–30)	27.1 ± 1.75 (23–30)	23.5 ± 2.10 (18–27)	$F = 303.47$; $df = 2, 392$; $P < .001$
CDR Sum of Boxes score†	0.03 ± 0.12 (0–1)	1.47 ± 0.87 (1–5)	4.27 ± 1.60 (2–9)	$F = 517.28$; $df = 2, 392$; $P < .001$
APOE risk‡	34 (24)	97 (55)	59 (70)	$\chi^2 = 51.38$, $df = 2$, $P < .001$

Note.—*APOE* = apolipoprotein E gene, MMSE = Mini-Mental State Examination.

* Data are numbers of subjects, and numbers in parentheses are percentages unless otherwise specified. Percentages were rounded.

† Data are the mean ± standard deviation, and numbers in parentheses are ranges unless otherwise specified.

‡ *APOE* risk was defined as the presence of the *APOE* ε4 allele. Data are numbers of subjects, and numbers in parentheses are percentages unless otherwise specified.

ment phase to optimize the MR imaging protocols for the relevant manufacturer platforms to maximize the scientific utility of the data and to ensure use of equivalent pulse sequences (44). Protocols are described in detail on the ADNI Research Cores page of the LONI Web site at *http://www.loni.ucla.edu/ADNI/Research/Cores/index.shtml* published in 2007. An example of a protocol for a 1.5-T MR system (Magnetom Sonata Syngo; Siemens Medical Solutions, Malvern, Pa), running version MR 2004A software, is the sagittal inversion-prepared three-dimensional T1-weighted gradient-echo sequence (magnetization-prepared rapid acquisition gradient echo or equivalent), with the following parameters: repetition time msec/echo time msec/inversion time msec, 2400/3.5/1000; flip angle, 8°; bandwidth, 180 Hz/pixel; field of view, 240 mm; matrix, 192 × 192; number of sections, 60; and section thickness, 1.2 mm. Two such images were collected per subject per visit. These raw Digital Imaging and Communications in Medicine MR images were downloaded from the ADNI Data page of the public ADNI site at the LONI Web site (*http://www.loni.ucla.edu/ADNI/Data/index.shtml*) published in 2007.

Locally, images were automatically corrected for spatial distortion caused by gradient nonlinearity (42) and B_1 field inhomogeneity (45). The two T1-weighted images from each subject were rigid-body aligned to each other and then averaged to improve signal-to-noise ratio and resampled to isotropic 1-mm voxels. Volumetric segmentation (23,24) and cortical surface reconstruction (19,20,22,25) methods that were based on the brain MR imaging software package mentioned before, optimized for use on large multisite data sets, were used. The automated whole-brain segmentation procedure (23,24) uses a probabilistic atlas and applies a Bayesian classification rule to assign a neuroanatomic label to each voxel. The atlas consists of a manually derived training set created by the Center for Morphometric Analysis (Massachusetts General Hospital, Harvard Medical School, Boston, Mass) from 40 non-ADNI subjects across the adult age range, including individuals with AD. Volumes for the hippocampus, amygdala, and ventricles were included in the present analysis. To control for individual differences in head size for volumetric measures, estimated total cranial vault volume was derived from the atlas scaling factor (46) on the basis of the transformation of the full brain mask into atlas space, as implemented in the software package. Automated volumetric segmentation required only qualitative review to ensure that there was no technical failure of the application. Failure occurred for 15 images (two for HC subjects, eight for subjects with MCI, and five for subjects with AD) because of extreme white matter disease or atrophy (eg, one case with extensive left temporal lobe loss such that the temporal horn of the lateral ventricle subsumed a large extent of the anterior temporal lobe). These subjects were excluded from analysis.

The cortical surface was reconstructed to measure thickness at each surface location, or vertex (19,20,22), to allow visualization of group differences at each vertex (21). The surface was parcellated into distinct regions of interest (ROIs) (25,27) (Fig 1). The cortical surface model was manually reviewed and edited for accuracy. Minimal editing was performed according to standard, objective rules, including correction of errors in removal of nonbrain areas and inclusion of white matter areas of hypointensity adjacent to the cortical ribbon. Qualitative review and editing was performed, with blinding to the diagnostic status, by one of three

Figure 1

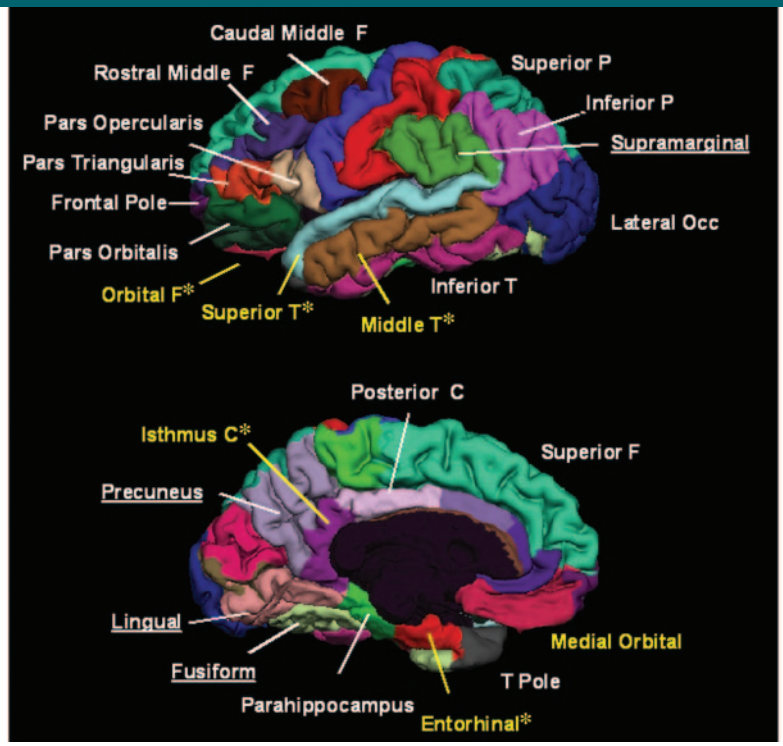

Figure 1: Pial representations of ROIs included as candidate input variables in the classifier. ROIs from both hemispheres were included; only left-hemisphere ROIs are shown here for convenience. Only labeled ROIs were included as candidate input variables in the classifier. In addition to ROIs visible on image, thickness of bank of superior temporal sulcus and volumes of hippocampus, amygdala, and lateral and inferior lateral ventricles were also included as candidate input variables. ROIs in yellow were selected as features in model. * = ROI in right hemisphere was included in model, *C* = cingulate, *F* = frontal gyrus, *Occ* = occipital gyrus, *P* = parietal gyrus, *T* = temporal gyrus.

technicians (including C.J.P.) trained and supervised by an expert neuroanatomist with more than 10 years of experience (C.F.). The technicians had a minimum of 4 months of experience reviewing brain MR images prior to their involvement in this project.

Qualitative review and editing required approximately 45 minutes per subject, with approximately 24 hours of computational time for image construction by using a dual quad-core central processing unit (Xeon E5420; Intel, Santa Clara, Calif) that had a processing speed of 2.50 GHz and 16 GB RAM. Use of several central processing units allowed the processing of images from multiple subjects to occur in parallel fashion.

Volumetric data were corrected for differences in head size by regressing the estimated total cranial vault volume (46). Effects of age and sex were regressed from all thickness and volumetric measures.

Statistical Analysis

Differences in age and educational level across the HC, MCI, and AD groups and between the MCI subgroups were assessed with analysis of variance; differences in the MMSE score (47), CDR Sum of Boxes score, and the Logical Memory I (Immediate Recall) and II (Delayed Recall) subscales of the Wechsler Memory Scale scores (for MCI subgroups) were assessed with analysis of covariance, controlling for the effects of age, sex, and educational level. Differences in sex distribution and genetic status were assessed with χ^2 tests of association, as were differences in the number of patients who had progression to a diagnosis of AD in the two MCI subgroups. In all analyses, a difference with a two-sided probability of $P < .05$ was considered significant.

To identify the pattern of regional atrophy that can be used to best discriminate AD subjects from HC subjects, stepwise linear discriminant analysis (LDA) employing the Wilks lambda method in a statistical software package (SPSS; SPSS, Chicago, Ill) was used. Candidate input variables comprised morphometric measures from 58 ROIs, including lateral ventricles, mesial temporal structures, and cortical association areas (Fig 1). Leave-one-out cross-validation minimized the inflation in sensitivity and specificity associated with use of the entire data set to train the classifier. With the statistical software package, feature selection occurs on the entire sample, not just the training sample, producing an optimistic bias in the estimation of classification performance (48). This bias was assessed by determining the classification accuracy achievable when feature selection and weighting were performed with the leave-one-out training samples only. To assess the overall discriminative power of each classifier, receiver operating characteristic curves were computed for each classifier, and the area under the curve was calculated. Statistical comparison of the areas under the curve of the partially and fully cross-validated classifiers was performed by using the method of Hanley and McNeil (49). The Cohen d effect size was calculated as the mean difference between LDA scores in HC subjects and subjects with AD, divided by the pooled standard deviation.

A classifier was trained on the data from all HC subjects and subjects with AD and then was applied to data from subjects with MCI. This produced a discriminant score, the atrophy score, for each individual with MCI, reflecting the degree to which the individual's MR image findings resembled the pattern of subjects with AD or the pattern of HC subjects. Classifier scores were generated with the assumption of equal prior group probabilities. The cutoff value for group categorization was chosen to minimize the error rate in classification of subjects with AD and HC subjects. A Kolmogorov-Smirnov test, with Lilliefors significance correction, was used to assess normality of the distribution of the atrophy scores for subjects with MCI. To assess differences in MMSE score over time in the resulting MCI subgroups, analyses of covariance were used, with age, sex, and educational level as covariates, MCI subgroup as a between-subject factor, and test interval (baseline and 6 and 12 months) as a within-subject factor, with Greenhouse-Geisser adjustment for violations of the assumption of sphericity. To assess significance of atrophy, relative to HC subjects, in the regions used to calculate the atrophy score, multivariate analysis of variance, followed by univariate analysis of variance with Bonferroni adjustments for multiple comparisons, was performed.

In a prospective manner, we examined whether the structural pattern measured at baseline in subjects with MCI was predictive of clinical decline by using stepwise linear regression, with 1-year change in MMSE score as the dependent variable and the following candidate predictor variables: atrophy score; genetic risk on the basis of the presence of the *APOE* ε4 allele; age; sex; educational level; and baseline scores on the clinical and neuropsychologic tests used for diagnosis in the ADNI, including the MMSE, CDR Sum of Boxes, and Logical Memory I (Immediate Recall) and II (Delayed Recall) scales of the Wechsler Memory Scale.

Because investigators in prior studies have found that measures of baseline atrophy in single structures, such as the hippocampus or entorhinal cortex (6,30–33), are predictive of clinical decline, Pearson correlations were calculated for 1-year change between MMSE score and the volumes of the left and right hippocampus, between the MMSE score and the thickness of the left and right entorhinal cortex, and between MMSE and the atrophy score.

Finally, to determine whether atrophy at baseline was associated with an increased rate of structural loss, repeated-measures analysis of covariance, while controlling for the effects of sex and age, was performed, with the MCI subgroup as a between-subject factor and the test interval (6 and 12 months) as a within-subject factor.

Results

The cross-validated results achieved with the statistical software package for LDA showed highly significant group discrimination between HC subjects

and those with AD (Table 2). When feature selection and weighting were restricted to the training sample, a lower sensitivity estimate and a significantly smaller area under the curve ($P < .001$) were obtained, although group separation was still excellent (Table 2, Fig 2), with a Cohen d effect size of 1.97. The receiver operating characteristic curve for this fully cross-validated model is shown in Figure 3.

A separate LDA, trained on data from all HC subjects and subjects with AD, was performed to classify the subjects with MCI who had the HC or AD imaging phenotype. The discriminant score from this model, the atrophy score, was computed from the following features and their weights: left hippocampal volume, $r = 0.709$; thickness of right entorhinal, $r = 0.597$; right middle temporal gyrus, $r = 0.506$; left bank of the superior temporal sulcus, $r = 0.453$; right isthmus cingulate, $r = 0.395$; right superior temporal gyrus, $r = 0.328$; left medial orbital frontal gyrus, $r = 0.269$; and right lateral orbital frontal gyrus, $r = 0.250$ (Fig 1), where the correlation is that of each measure with the standardized canonical discriminant function. Distribution of the atrophy score for the participants with MCI is shown in Figure 4. Participants with MCI who had the AD phenotype had a pattern of regional atrophy nearly identical to that of the AD group, even in regions that did not contribute to the atrophy score. Subjects with MCI who had the HC phenotype displayed little atrophy (Fig 5). Relative to HC subjects, subjects with MCI who had the AD phenotype had significant atrophy in all eight areas used to calculate the atrophy score (Bonferroni-adjusted P values of .001 or less for all comparisons), whereas subjects with MCI who had the HC phenotype had significant atrophy in the hippocampus ($P = .008$) and middle temporal gyrus ($P = .047$) only. Demographic and clinical characteristics of the two MCI subgroups are shown in Table 3. Relative to individuals with the HC phenotype, those with the AD phenotype had higher CDR Sum of Boxes and lower verbal memory scores.

For the 160 participants with MCI for whom clinical follow-up data were available, those with the AD phenotype showed significant 1-year decline in MMSE score, whereas those with the HC phenotype remained stable (testing interval according to predicted group interaction; $F = 8.67$; $df = 2, 310$; $P < .001$) (Fig 6). Atrophy score was the primary predictor for this decline ($R = 0.39$; $F = 28.36$; $df = 1, 158$; $P < .001$). However, prediction improved with ad-

Table 2

Comparison of Classification Accuracy of Linear Discriminant Models with Partial or Full Cross Validation

Model	Overall Accuracy ($n = 223$)*	Sensitivity ($n = 84$)*	Specificity ($n = 139$)*	Area under the Curve†
Partially cross validated	92 (205)	89 (75)	94 (130)	0.968 ± 0.011
95% Confidence interval	87.3, 95.0	80.2, 95.3	87.7, 97.2	0.947, 0.989
Fully cross validated	89 (199)	83 (70)	93 (129)	0.915 ± 0.022‡
95% Confidence interval	84.2, 92.8	72.9, 90.5	87.1, 96.8	0.872, 0.958

Note.—This leave-one-out analysis included 139 HC subjects and 84 subjects with AD.

* Data are percentages, and numbers in parentheses were used to calculate the percentages. Percentages were rounded.

† Data are the mean ± standard error of the mean unless otherwise specified.

‡ $P < .001$, comparison of the area under the curve for the two models.

Figure 2

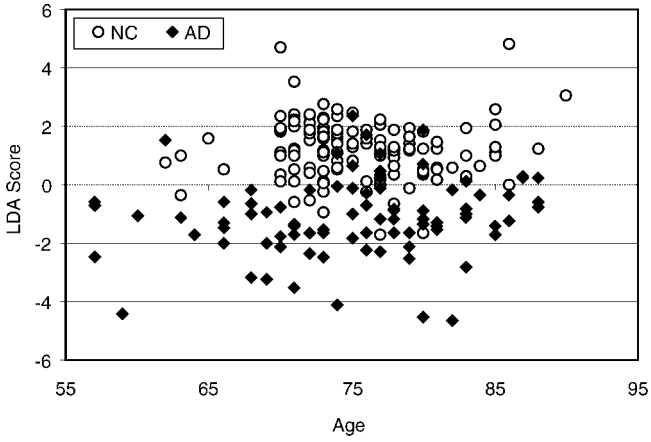

Figure 2: Graph shows separation of HC *(NC)* subjects and subjects with AD on basis of LDA score as function of age. Results of fully cross-validated discriminant model are shown. Discriminant model assumed equal prior group probabilities. Individuals were classified as HC subjects if their scores were above −0.10. This cutoff score was chosen on basis of receiver operating characteristic curve to maximize overall classification accuracy.

Figure 3

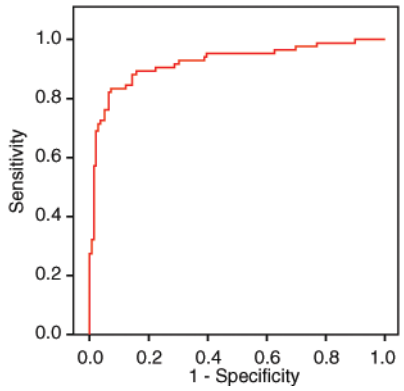

Figure 3: Receiver operating characteristic curve for fully cross-validated discriminant model.

Figure 4

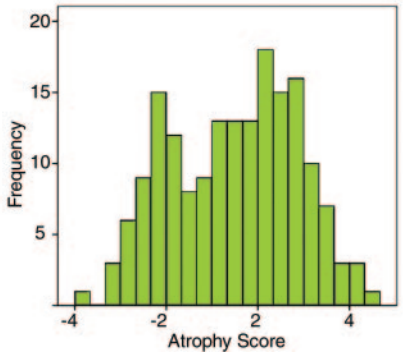

Figure 4: Graph shows distribution of atrophy scores used to classify subjects with MCI. MCI atrophy score was derived from LDA trained on data from all HC subjects and subjects with AD. Discriminant model assumed equal prior group probabilities. Individuals were classified as having HC phenotype if their scores were above −0.33. Cutoff score was chosen to maximize overall accuracy of classifying HC subjects and subjects with AD on whom this model was trained. Average atrophy score for subjects with MCI was −0.50. Atrophy score is not normally distributed (Kolmogorov-Smirnov test = 0.73, $df = 175$, $P = .025$) but shows evidence of bimodal distribution.

Figure 5

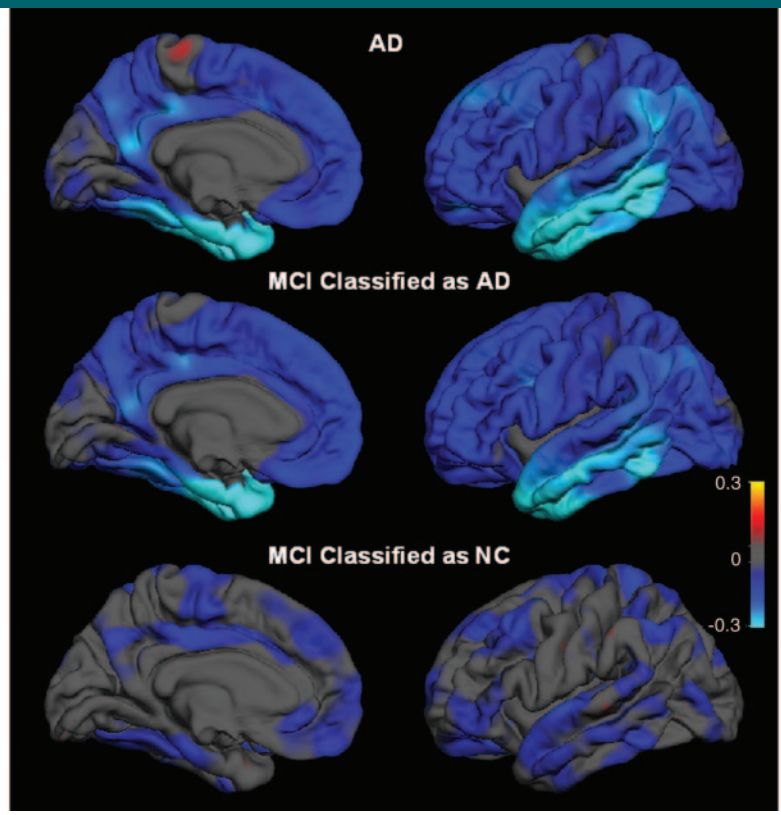

Figure 5: Average differences in thickness for subjects with AD and MCI relative to HC *(NC)*. Top: HC subjects versus subjects with AD. Middle: HC subjects versus subjects with MCI who had AD imaging phenotype. Bottom: HC subjects versus subjects with MCI who had HC imaging phenotype. Right: Lateral views. Left: Mesial views. Blue areas indicate regions of thinning with disease. Scale reflects thickness ranging from −0.3-mm thickness (bright blue or cyan) to +0.3-mm thickness (yellow).

dition of *APOE* status ($R = 0.442$; $F = 19.10$; $df = 2, 157$; $P < .001$), MMSE results ($R = 0.467$; $F = 14.51$; $df = 4, 156$; $P < .001$), and Logical Memory II (Delayed Recall) subscale of the Wechsler Memory Scale scores ($R = 0.498$; $F = 12.77$; $df = 4, 155$; $P < .001$).

The atrophy score showed a higher correlation with 1-year clinical decline in subjects with MCI ($r = 0.39$, $P < .001$) than did left ($r = 0.29$, $P < .001$) or right ($r = 0.33$, $P < .001$) hippocampal volumes alone or thickness of left ($r = 0.16$, $P < .05$) or right ($r = 0.22$, $P < .01$) entorhinal cortices alone.

Of the 128 HC subjects with 1-year follow-up diagnostic data, two had progression to a diagnosis of MCI but none had progression to a diagnosis of probable AD. Of the 160 subjects with MCI in whom follow-up data were available, four reverted to normal cognitive status (three of whom had the HC imaging phenotype) and 33 had progression to probable AD. Those who had progression were significantly more likely to have the AD phenotype ($n = 26$) than the HC phenotype ($n = 7$) ($\chi^2 = 12.67$, $df = 1$, $P < .001$): The conversion rate among subjects with MCI who had AD atrophy was 29% (26 of 89) versus 8% (seven of 86) for the subjects with MCI who had the HC phenotype.

For the 129 participants with MCI in whom follow-up processed MR imaging data were available, those with AD atrophy showed significantly greater structural loss over time than those without ($F = 12.0$; $df = 1, 125$; $P = .001$), particularly in mesial and lateral middle temporal areas (group according to region interaction; $F = 5.62$; $df = 7, 875$; $P < .001$) (Fig 7).

Discussion

Our study was designed to determine whether individually specific quantitative structural neuroimaging measures could be used to detect mild AD and to predict decline in individuals with MCI. We found that a pattern of regional atrophy could be identified that could be used to discriminate individuals with mild AD from HC subjects, with high sensitivity and specificity. Sensitivity was on par with clinical diagnostic accuracy: Accuracy of AD that is based on histopathologic verification ranges from 85% to 90% (50–52). Although investigators in some prior studies have reported classification accuracy values ranging from 90% to 100% on the basis of MR imaging measures, they used smaller sample sizes (16,31,53–55), included AD groups with more severe impairment (53–55), or did not report fully cross-validated results (16,31,53,54). Failure to cross-validate results produces an optimis-

tic bias in classification accuracy (48,56), as shown in our study in the decrease in sensitivity that occurred when full cross-validation was used.

Application of the discriminant model developed with data from HC subjects and subjects with AD and applied to subjects with MCI revealed that a subgroup of individuals with MCI could be identified who displayed a regional atrophy pattern similar to that in AD patients. Expression of this pattern at baseline was predictive of clinical decline. Similar results have recently been reported on a smaller subset of the ADNI cohort, in which a nonlinear classifier was applied to voxel-based morphometric data to discriminate HC from AD data (16). Although that study reported higher classification accuracy than that achieved in our study, the best combination of free parameters in the support vector machine approach to classification used in that report is partially determined by the left-out data samples (57), an approach that leads to overfitting the data when the number of samples is much smaller than the number of potential features. The pattern of atrophy that aided in the discrimination of subjects with AD from HC subjects in that study was spatially complex, involving temporal, frontal, and posterior cingulate regions. As observed here, expression of the AD atrophy pattern at baseline was predictive of 1-year MMSE score decline in subjects with MCI (16). We further show, however, that expression of the AD pattern at baseline also was associated with a higher risk of progression to a diagnosis of probable AD and with a greater rate of progressive structural atrophy over a 1-year period.

The pattern that best aided in the discrimination of HC subjects from subjects with AD and that was predictive of decline in subjects with MCI involved atrophy, relative to HC subjects, in mesial temporal, lateral temporal, isthmus cingulate, and orbitofrontal regions. Mesial temporal structures have long been known to be implicated early in AD, and atrophy in these structures has been found to be predictive of disease progression (6,13,31,33,35). Lateral temporal areas, particularly middle and inferior temporal gyri, have been implicated in the progression of AD (8,15,58,59). Atrophy of the superior temporal gyrus, however, has typically been observed only after a diagnosis of probable AD (58,59). We observed significant atrophy in this area in the subgroup of individuals with MCI who have AD atrophy, as did Fan et al (16), suggesting that atrophy of the superior temporal gyrus can occur prior to a diagnosis of probable AD and is associated with a higher risk of imminent clinical decline.

We also observed atrophy in the isthmus cingulate (the caudal portion of the posterior cingulate) and orbitofrontal areas in subjects with MCI who have phenotypic AD atrophy. Posterior cingulate and frontal atrophy have been inconsistently observed in MCI and mild AD in both cross-sectional and longitudinal studies (10,14–16,58–62). Methodological differences likely contribute to these discrepant findings. Nevertheless, the growing body of evidence suggests that there is substantial widespread cortical atrophy in preclinical stages of AD and that involvement of areas outside the mesial temporal lobe, including lateral temporal, posterior cingulate, and frontal areas, may be predictive of a more rapid course of disease progression.

Subjects with MCI who had AD atrophy had greater functional and memory impairment at baseline than those who did not. Nevertheless, the atrophy score was the primary predictor of clinical decline, with additional contribu-

Table 3

Demographics and Clinical and Neuropsychologic Characterization of Participants with MCI and HC or AD Imaging Phenotype

Group	HC Pattern (n = 86)	AD Pattern (n = 89)	Statistical Comparison
Age (y)*	74.50 ± 7.68	74.9 ± 7.14	F = 0.10; df = 1, 173; P = .75
Sex			
Male†	67 (78)	56 (63)	χ^2 = 4.70, df = 1, P = .03
Female†	19 (22)	33 (37)	. . .
Education (y)*	15.8 ± 2.94	16.2 ± 2.58	F = 0.82; df = 1, 173; P = .37
MMSE score‡	27.3 ± 1.78 (24–30)	26.8 ± 1.68 (23–30)	F = 5.2; df = 1, 170; P = .024
CDR Sum of Boxes score‡	1.34 ± 0.74 (0.5–3.5)	1.61 ± 0.96 (0.5–4.5)	F = 5.01; df = 1, 170; P = .026
APOE risk§	44 (51)	53 (60)	χ^2 = 1.25, df = 1, P = .264
Logical Memory I‖	8.00 ± 3.03	6.03 ± 2.73	F = 26.53; df = 1, 170; P < .001
Logical Memory II**	4.721 ± 2.42	2.67 ± 2.64	F = 32.66; df = 1, 170; P < .001

* Data are the mean ± standard deviation unless otherwise specified.

† Data are numbers of participants, and numbers in parentheses are percentages unless otherwise specified. Percentages were rounded.

‡ Data are the mean ± standard deviation, and numbers in parentheses are ranges unless otherwise specified.

§ *APOE* risk was defined as the presence of the *APOE* ε4 allele.

‖ This test is the subscale for Immediate Recall of the Wechsler Memory Scale. Data are the mean ± standard deviation unless otherwise specified.

** This test is the subscale for Delayed Recall of the Wechsler Memory Scale. Data are the mean ± standard deviation unless otherwise specified.

Figure 6

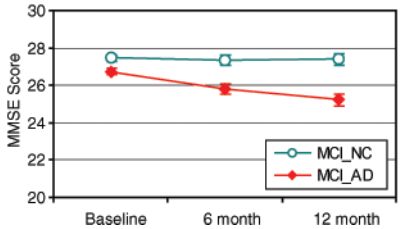

Figure 6: Graph shows MMSE score at baseline and at 6- and 12-month follow-up as function of neuroimaging phenotype in participants with MCI; 1-year clinical follow-up data were available for 160 participants with MCI. MCI group with AD phenotype *(MCI_AD)* (n = 72) had significant decline over time; MCI group with HC phenotype *(MCI_NC)* (n = 88) did not.

Figure 7

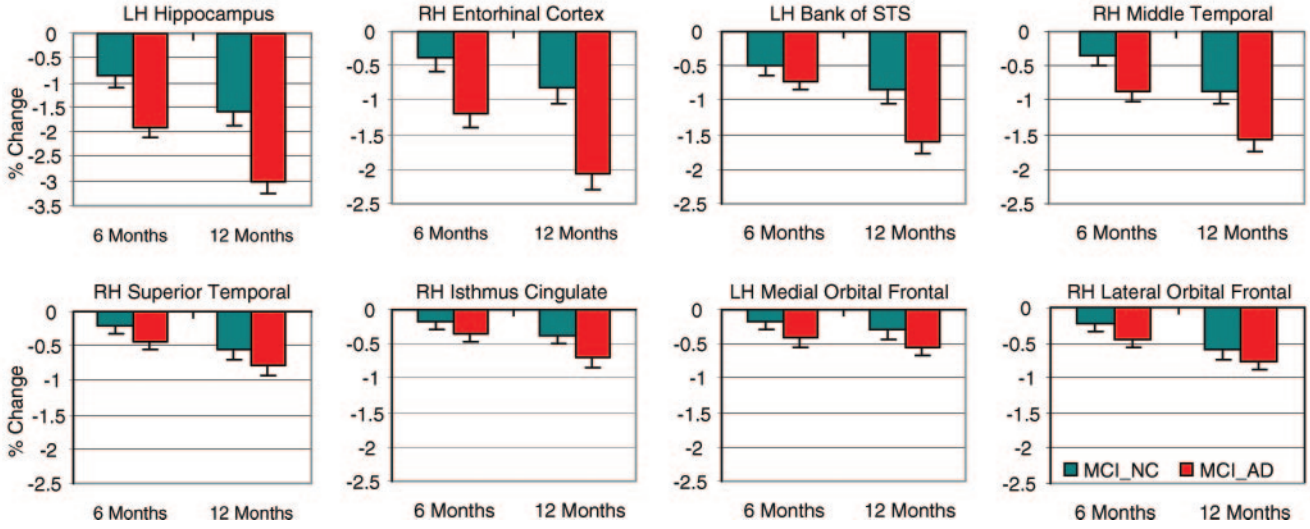

Figure 7: Percentage change in volume for HC subjects or thickness at 6- and 12-month follow-up sessions for subjects with MCI who had HC and AD imaging phenotypes; 1-year follow-up MR imaging data were available for 129 participants with MCI. Percentage changes are shown for eight ROIs used to compute atrophy score. Red bars indicate subjects with MCI who had AD phenotype *(MCI_AD)* ($n = 66$); significantly greater structural loss was observed in these subjects than in those who had HC phenotype *(MCI_NC),* signified by teal bars ($n = 63$), particularly in mesial and lateral middle temporal areas. Group differences in structural loss for superior temporal gyrus, isthmus cingulate, and frontal ROIs (bottom row) were not significant. *LH* = left hemisphere, *RH* = right hemisphere, *STS* = superior temporal sulcus.

tion to predictive value provided by the *APOE* status, baseline MMSE results, and Logical Memory II (Delayed Recall) subscale of the Wechsler Memory Scale scores. This datum contrasts with the datum in a recent report that indicated that whole-brain, ventricular, entorhinal, and hippocampal volumes did not provide additional predictive information about clinical decline beyond that attainable with clinical measures (63) and shows the value of examining individually specific brain regions beyond the mesial temporal lobe. Future analysis by using the full neuropsychologic battery in the complete ADNI cohort will more formally address the comparative value of clinical versus morphometric measures in the prediction of disease progression.

Expression of the AD pattern at baseline in MCI was associated with progressive structural loss, as well as with clinical decline. This increased rate of atrophy was observed primarily in mesial and lateral temporal areas and is consistent with prior findings of accelerated atrophy rates in these areas in MCI (10,11,15,34,35,58,59,64,65). These findings suggest that measures of structural change in mesial and lateral temporal areas may be promising biomarkers for the assessment of the capability of a treatment to halt the progressive structural loss that accompanies clinical decline in MCI.

Limitations of this study include the following: *(a)* This study lacked histopathologic verification of AD and HC status. *(b)* There was an atypical bias, a bias that is characteristic of the larger ADNI cohort, toward male subjects in the MCI group; this bias was unlikely to have negatively affected the results because the classifier used to derive the atrophy score was trained on data in HC subjects and subjects with AD, and these groups did not show strong sex bias. *(c)* The ADNI is ongoing, and current follow-up data are limited and preliminary. *(d)* The time frame of follow-up in the current study (1 year) is too short to obtain a sufficient number of subjects with a status progressing to a diagnosis of probable AD to assess the sensitivity and specificity of predicting progression on the basis of the atrophy score. *(e)* Intrarater and interrater reliability of the cortical editing procedures have not yet been formally assessed. Because editing included correction of instances in which the gray matter–white matter boundary invaded white matter to include white matter areas of hypointensity in the cortical ribbon, the thickness measures in cases of white matter disease may be less reliable, although subjects with extreme white matter disease were excluded from analysis.

In conclusion, quantitative structural MR imaging measures can be used to identify a pattern of regional atrophy at baseline in subjects with MCI that is predictive of a 1-year clinical decline. Such an improvement in predictive prognostic information could be valuable for individual patient treatment, particularly when aggressive new treatments that may prevent or delay AD become available. Currently, such information could provide an important enrichment strategy for the design of large-scale clinical trials, enabling them to identify a more homogeneous cohort of individuals with MCI who are at

high risk of imminent decline, allowing for smaller sample sizes and shorter trial durations.

Acknowledgments: ADNI is funded by the National Institute on Aging, the National Institute of Biomedical Imaging and Bioengineering, and through generous contributions from the following: Pfizer, Wyeth Research, Bristol-Myers Squibb, Eli Lilly, GlaxoSmithKline, Merck, AstraZeneca, Novartis Pharmaceuticals, Alzheimer's Association, Eisai Global Clinical Development, Elan, Forest Laboratories, and the Institute for the Study of Aging, with participation from the U.S. Food and Drug Administration. Industry partnerships are coordinated through the Foundation for the National Institutes of Health. The grantee organization is the Northern California Institute for Research and Education, and the study is coordinated by the Alzheimer Disease Cooperative Study at the University of California, San Diego, Calif. ADNI data are disseminated by the Laboratory of Neuro Imaging at the University of California, Los Angeles, Calif.

We thank Robin G. Jennings, BS, Michele E. Perry, MS, and Elaine H. Wu, BS, for downloading and preprocessing the ADNI MR imaging data.

References

1. Morris JC, Storandt M, Miller JP, et al. Mild cognitive impairment represents early-stage Alzheimer disease. Arch Neurol 2001;58:397–405.
2. Petersen RC. Mild cognitive impairment as a diagnostic entity. J Intern Med 2004;256:183–194.
3. Petersen RC, Bennett D. Mild cognitive impairment: is it Alzheimer's disease or not? J Alzheimers Dis 2005;7:241–245.
4. Mueller SG, Weiner MW, Thal LJ, et al. Ways toward an early diagnosis in Alzheimer's disease: the Alzheimer's Disease Neuroimaging Initiative (ADNI). Alzheimers Dement 2005;1:55–66.
5. Ramani A, Jensen JH, Helpern JA. Quantitative MR imaging in Alzheimer disease. Radiology 2006;241:26–44.
6. Jack CR Jr, Petersen RC, Xu YC, et al. Prediction of AD with MRI-based hippocampal volume in mild cognitive impairment. Neurology 1999;52:1397–1403.
7. Visser PJ, Scheltens P, Verhey FR, et al. Medial temporal lobe atrophy and memory dysfunction as predictors for dementia in subjects with mild cognitive impairment. J Neurol 1999;246:477–485.
8. Convit A, de Asis J, de Leon MJ, Tarshish CY, De Santi S, Rusinek H. Atrophy of the medial occipitotemporal, inferior, and middle temporal gyri in non-demented elderly predict decline to Alzheimer's disease. Neurobiol Aging 2000;21:19–26.
9. Killiany RJ, Gomez-Isla T, Moss M, et al. Use of structural magnetic resonance imaging to predict who will get Alzheimer's disease. Ann Neurol 2000;47:430–439.
10. Chetelat G, Landeau B, Eustache F, et al. Using voxel-based morphometry to map the structural changes associated with rapid conversion in MCI: a longitudinal MRI study. Neuroimage 2005;27:934–946.
11. Jack CR Jr, Shiung MM, Weigand SD, et al. Brain atrophy rates predict subsequent clinical conversion in normal elderly and amnestic MCI. Neurology 2005;65:1227–1231.
12. Apostolova LG, Dutton RA, Dinov ID, et al. Conversion of mild cognitive impairment to Alzheimer disease predicted by hippocampal atrophy maps. Arch Neurol 2006;63:693–699.
13. Devanand DP, Pradhaban G, Liu X, et al. Hippocampal and entorhinal atrophy in mild cognitive impairment: prediction of Alzheimer disease. Neurology 2007;68:828–836.
14. Hamalainen A, Tervo S, Grau-Olivares M, et al. Voxel-based morphometry to detect brain atrophy in progressive mild cognitive impairment. Neuroimage 2007;37:1122–1131.
15. Whitwell JL, Shiung MM, Przybelski SA, et al. MRI patterns of atrophy associated with progression to AD in amnestic mild cognitive impairment. Neurology 2008;70:512–520.
16. Fan Y, Batmanghelich N, Clark CM, Davatzikos C. Spatial patterns of brain atrophy in MCI patients, identified via high-dimensional pattern classification, predict subsequent cognitive decline. Neuroimage 2008;39:1731–1743.
17. Ashburner J, Csernansky JG, Davatzikos C, Fox NC, Frisoni GB, Thompson PM. Computer-assisted imaging to assess brain structure in healthy and diseased brains. Lancet Neurol 2003;2:79–88.
18. Ashburner J, Friston KJ. Voxel-based morphometry: the methods. Neuroimage 2000;11:805–821.
19. Dale AM, Sereno MI. Improved localization of cortical activity by combining EEG and MEG with MRI cortical surface reconstruction: a linear approach. J Cogn Neurosci 1993;5:162–176.
20. Dale AM, Fischl B, Sereno MI. Cortical surface-based analysis. I. Segmentation and surface reconstruction. Neuroimage 1999;9:179–194.
21. Fischl B, Dale AM. Measuring the thickness of the human cerebral cortex from magnetic resonance images. Proc Natl Acad Sci U S A 2000;97:11050–11055.
22. Fischl B, Sereno MI, Dale AM. Cortical surface-based analysis. II. Inflation, flattening, and a surface-based coordinate system. Neuroimage 1999;9:195–207.
23. Fischl B, Salat DH, Busa E, et al. Whole brain segmentation: automated labeling of neuroanatomical structures in the human brain. Neuron 2002;33:341–355.
24. Fischl B, Salat DH, van der Kouwe AJ, et al. Sequence-independent segmentation of magnetic resonance images. Neuroimage 2004;23(suppl 1):S69–S84.
25. Fischl B, Van Der Kouwe A, Destrieux C, et al. Automatically parcellating the human cerebral cortex. Cereb Cortex 2004;14:11–22.
26. Rosas HD, Liu AK, Hersch S, et al. Regional and progressive thinning of the cortical ribbon in Huntington's disease. Neurology 2002;58:695–701.
27. Desikan RS, Segonne F, Fischl B, et al. An automated labeling system for subdividing the human cerebral cortex on MRI scans into gyral based regions of interest. Neuroimage 2006;31:968–980.
28. Fjell AM, Walhovd KB, Reinvang I, et al. Selective increase of cortical thickness in high-performing elderly: structural indices of optimal cognitive aging. Neuroimage 2006;29:984–994.
29. Du AT, Schuff N, Kramer JH, et al. Different regional patterns of cortical thinning in Alzheimer's disease and frontotemporal dementia. Brain 2007;130:1159–1166.
30. de Leon MJ, Convit A, DeSanti S, et al. Contribution of structural neuroimaging to the early diagnosis of Alzheimer's disease. Int Psychogeriatr 1997;9(suppl 1):183–190.
31. Killiany RJ, Hyman BT, Gomez-Isla T, et al. MRI measures of entorhinal cortex vs hippocampus in preclinical AD. Neurology 2002;58:1188–1196.
32. den Heijer T, Geerlings MI, Hoebeek FE, Hofman A, Koudstaal PJ, Breteler MM. Use of hippocampal and amygdalar volumes on magnetic resonance imaging to predict dementia in cognitively intact elderly people. Arch Gen Psychiatry 2006;63:57–62.
33. DeToledo-Morrell L, Stoub TR, Bulgakova M, et al. MRI-derived entorhinal volume is a good predictor of conversion from MCI to AD. Neurobiol Aging 2004;25:1197–1203.
34. Jack CR Jr, Petersen RC, Xu Y, et al. Rates of hippocampal atrophy correlate with

change in clinical status in aging and AD. Neurology 2000;55:484–489.

35. Stoub TR, Bulgakova M, Leurgans S, et al. MRI predictors of risk of incident Alzheimer disease: a longitudinal study. Neurology 2005;64:1520–1524.

36. Galton CJ, Patterson K, Graham K, et al. Differing patterns of temporal atrophy in Alzheimer's disease and semantic dementia. Neurology 2001;57:216–225.

37. van de Pol LA, Hensel A, van der Flier WM, et al. Hippocampal atrophy on MRI in frontotemporal lobar degeneration and Alzheimer's disease. J Neurol Neurosurg Psychiatry 2006;77:439–442.

38. Mueller SG, Weiner MW, Thal LJ, et al. The Alzheimer's disease neuroimaging initiative. Neuroimaging Clin N Am 2005;15:869–877, xi–xii.

39. Hughes CP, Berg L, Danziger WL, Coben LA, Martin RL. A new clinical scale for the staging of dementia. Br J Psychiatry 1982; 140:566–572.

40. McKhann G, Drachman D, Folstein M, Katzman R, Price D, Stadlan EM. Clinical diagnosis of Alzheimer's disease: report of the NINCDS-ADRDA Work Group under the auspices of Department of Health and Human Services Task Force on Alzheimer's Disease. Neurology 1984;34:939–944.

41. Fennema-Notestine C, Ozyurt IB, Clark CP, et al. Quantitative evaluation of automated skull-stripping methods applied to contemporary and legacy images: effects of diagnosis, bias correction, and slice location. Hum Brain Mapp 2006;27:99–113.

42. Jovicich J, Czanner S, Greve D, et al. Reliability in multi-site structural MRI studies: effects of gradient non-linearity correction on phantom and human data. Neuroimage 2006;30:436–443.

43. Han X, Jovicich J, Salat D, et al. Reliability of MRI-derived measurements of human cerebral cortical thickness: the effects of field strength, scanner upgrade and manufacturer. Neuroimage 2006;32:180–194.

44. Jack CR Jr, Bernstein MA, Fox NC, et al. The Alzheimer's disease neuroimaging initiative (ADNI): MRI methods. J Magn Reson Imaging 2008;27:685–691.

45. Sled JG, Zijdenbos AP, Evans AC. A nonparametric method for automatic correction of intensity nonuniformity in MRI data. IEEE Trans Med Imaging 1998;17:87–97.

46. Buckner RL, Head D, Parker J, et al. A unified approach for morphometric and functional data analysis in young, old, and demented adults using automated atlas-based head size normalization: reliability and validation against manual measurement of total intracranial volume. Neuroimage 2004;23: 724–738.

47. Folstein MF, Folstein SE, McHugh PR. "Mini-mental state": a practical method for grading the cognitive state of patients for the clinician. J Psychiatr Res 1975;12:189–198.

48. Spycher S, Nendza M, Gasteiger J. Comparison of different classification methods applied to a mode of toxic action data set. QSAR Comb Sci 2004;23:779–791.

49. Hanley JA, McNeil BJ. A method of comparing the areas under receiver operating characteristic curves derived from the same cases. Radiology 1983;148:839–843.

50. Gearing M, Mirra SS, Hedreen JC, Sumi SM, Hansen LA, Heyman A. The Consortium to Establish a Registry for Alzheimer's Disease (CERAD). X. Neuropathology confirmation of the clinical diagnosis of Alzheimer's disease. Neurology 1995;45:461–466.

51. Mok W, Chow TW, Zheng L, Mack WJ, Miller C. Clinicopathological concordance of dementia diagnoses by community versus tertiary care clinicians. Am J Alzheimers Dis Other Demen 2004;19:161–165.

52. Schneider JA, Arvanitakis Z, Bang W, Bennett DA. Mixed brain pathologies account for most dementia cases in community-dwelling older persons. Neurology 2007;69:2197–2204.

53. Juottonen K, Laakso MP, Partanen K, Soininen H. Comparative MR analysis of the entorhinal cortex and hippocampus in diagnosing Alzheimer disease. AJNR Am J Neuroradiol 1999;20:139–144.

54. Callen DJ, Black SE, Gao F, Caldwell CB, Szalai JP. Beyond the hippocampus: MRI volumetry confirms widespread limbic atrophy in AD. Neurology 2001;57:1669–1674.

55. Lerch JP, Pruessner J, Zijdenbos AP, et al. Automated cortical thickness measurements from MRI can accurately separate Alzheimer's patients from normal elderly controls. Neurobiol Aging 2008;29:23–30.

56. Schulerud H, Albregtsen F. Many are called, but few are chosen: feature selection and error estimation in high dimensional spaces. Comput Methods Programs Biomed 2004; 73:91–99.

57. Fan Y, Shen D, Gur RC, Gur RE, Davatzikos C. COMPARE: classification of morphological patterns using adaptive regional elements. IEEE Trans Med Imaging 2007;26: 93–105.

58. Scahill RI, Schott JM, Stevens JM, Rossor MN, Fox NC. Mapping the evolution of regional atrophy in Alzheimer's disease: unbiased analysis of fluid-registered serial MRI. Proc Natl Acad Sci U S A 2002;99:4703–4707.

59. Whitwell JL, Przybelski SA, Weigand SD, et al. 3D maps from multiple MRI illustrate changing atrophy patterns as subjects progress from mild cognitive impairment to Alzheimer's disease. Brain 2007;130:1777–1786.

60. Singh V, Chertkow H, Lerch JP, Evans AC, Dorr AE, Kabani NJ. Spatial patterns of cortical thinning in mild cognitive impairment and Alzheimer's disease. Brain 2006;129: 2885–2893.

61. Pengas G, Hodges JR, Watson P, Nestor PJ. Focal posterior cingulate atrophy in incipient Alzheimer's disease. Neurobiol Aging doi: 10.1016/j.neurobiolaging.2008.03.014. Published May 2, 2008. Accessed May 15, 2008.

62. Pennanen C, Testa C, Laakso MP, et al. A voxel based morphometry study on mild cognitive impairment. J Neurol Neurosurg Psychiatry 2005;76:11–14.

63. Fleisher AS, Sowell BB, Taylor C, Gamst AC, Petersen RC, Thal LJ. Clinical predictors of progression to Alzheimer disease in amnestic mild cognitive impairment. Neurology 2007;68:1588–1595.

64. Jack CR Jr, Slomkowski M, Gracon S, et al. MRI as a biomarker of disease progression in a therapeutic trial of milameline for AD. Neurology 2003;60:253–260.

65. Jack CR Jr, Shiung MM, Gunter JL, et al. Comparison of different MRI brain atrophy rate measures with clinical disease progression in AD. Neurology 2004;62:591–600.

Radiology 2009

This is your reprint order form or pro forma invoice

(Please keep a copy of this document for your records.)

Reprint order forms and purchase orders or prepayments must be received 72 hours after receipt of form either by mail or by fax at 410-820-9765. It is the policy of Cadmus Reprints to issue one invoice per order. **Please print clearly**.

Author Name _____
Title of Article _____
Issue of Journal_____ Reprint # _____ Publication Date _____
Number of Pages_____ KB # _____ Symbol Radiology
Color in Article? Yes / No (Please Circle)

Please include the journal name and reprint number or manuscript number on your purchase order or other correspondence.

Order and Shipping Information

Reprint Costs **(Please see page 2 of 2 for reprint costs/fees.)**

_____ Number of reprints ordered $_____
_____ Number of color reprints ordered $_____
_____ Number of covers ordered $_____
Subtotal $_____
Taxes $_____

(*Add appropriate sales tax for Virginia, Maryland, Pennsylvania, and the District of Columbia or Canadian GST to the reprints if your order is to be shipped to these locations*.)

First address included, add $32 for each additional shipping address $_____

TOTAL $_____

Shipping Address **(cannot ship to a P.O. Box) Please Print Clearly**

Name _____
Institution _____
Street _____
City _____ State _____ Zip _____
Country _____
Quantity_____ Fax _____
Phone: Day _____ Evening _____
E-mail Address _____

Additional Shipping Address* **(cannot ship to a P.O. Box)**

Name _____
Institution _____
Street _____
City _____ State _____ Zip _____
Country _____
Quantity _____ Fax _____
Phone: Day _____ Evening _____
E-mail Address _____

** Add $32 for each additional shipping address*

Payment and Credit Card Details

Enclosed: Personal Check _____
Credit Card Payment Details _____

Checks must be paid in U.S. dollars and drawn on a U.S. Bank.

Credit Card: __ VISA __ Am. Exp. __ MasterCard
Card Number _____
Expiration Date_____
Signature: _____

Please send your order form and prepayment made payable to:

Cadmus Reprints
P.O. Box 751903
Charlotte, NC 28275-1903

Note: Do not send express packages to this location, PO Box.

FEIN #:541274108

Invoice or Credit Card Information

Invoice Address **Please Print Clearly**

Please complete Invoice address as it appears on credit card statement

Name _____
Institution _____
Department _____
Street _____
City _____ State _____ Zip _____
Country _____
Phone _____ Fax _____
E-mail Address _____

Cadmus will process credit cards and *Cadmus Journal Services* will appear on the credit card statement.

If you don't mail your order form, you may fax it to 410-820-9765 with your credit card information.

Signature _____ Date _____

Signature is required. By signing this form, the author agrees to accept the responsibility for the payment of reprints and/or all charges described in this document.

RB-1/01/09

Radiology 2009

Black and White Reprint Prices

Domestic (USA only)						
# of Pages	50	100	200	300	400	500
1-4	$239	$260	$285	$303	$323	$340
5-8	$379	$420	$455	$491	$534	$572
9-12	$507	$560	$651	$684	$748	$814
13-16	$627	$698	$784	$868	$954	$1,038
17-20	$755	$845	$947	$1,064	$1,166	$1,272
21-24	$878	$985	$1,115	$1,250	$1,377	$1,518
25-28	$1,003	$1,136	$1,294	$1,446	$1,607	$1,757
29-32	$1,128	$1,281	$1,459	$1,632	$1,819	$2,002
Covers	$149	$164	$219	$275	$335	$393

International (includes Canada and Mexico)						
# of Pages	50	100	200	300	400	500
1-4	$299	$314	$367	$429	$484	$546
5-8	$470	$502	$616	$722	$838	$949
9-12	$637	$687	$852	$1,031	$1,190	$1,369
13-16	$794	$861	$1,088	$1,313	$1,540	$1,765
17-20	$963	$1,051	$1,324	$1,619	$1,892	$2,168
21-24	$1,114	$1,222	$1,560	$1,906	$2,244	$2,588
25-28	$1,287	$1,412	$1,801	$2,198	$2,607	$2,998
29-32	$1,441	$1,586	$2,045	$2,499	$2,959	$3,418
Covers	$211	$224	$324	$444	$558	$672

Color Reprint Prices

Domestic (USA only)						
# of Pages	50	100	200	300	400	500
1-4	$247	$267	$385	$515	$650	$780
5-8	$297	$435	$655	$923	$1194	$1467
9-12	$445	$563	$926	$1,339	$1,748	$2,162
13-16	$587	$710	$1,201	$1,748	$2,297	$2,843
17-20	$738	$858	$1,474	$2,167	$2,846	$3,532
21-24	$888	$1,005	$1,750	$2,575	$3,400	$4,230
25-28	$1,035	$1,164	$2,034	$2,986	$3,957	$4,912
29-32	$1,186	$1,311	$2,302	$3,402	$4,509	$5,612
Covers	$149	$164	$219	$275	$335	$393

International (includes Canada and Mexico))						
# of Pages	50	100	200	300	400	500
1-4	$306	$321	$467	$642	$811	$986
5-8	$387	$517	$816	$1,154	$1,498	$1,844
9-12	$574	$689	$1,157	$1,686	$2,190	$2,717
13-16	$754	$874	$1,506	$2,193	$2,883	$3,570
17-20	$710	$1,063	$1,852	$2,722	$3,572	$4,428
21-24	$1,124	$1,242	$2,195	$3,231	$4,267	$5,300
25-28	$1,320	$1,440	$2,541	$3,738	$4,957	$6,153
29-32	$1,498	$1,616	$2,888	$4,269	$5,649	$7028
Covers	$211	$224	$324	$444	$558	$672

Minimum order is 50 copies. For orders larger than 500 copies, please consult Cadmus Reprints at 800-407-9190.

Reprint Cover

Cover prices are listed above. The cover will include the publication title, article title, and author name in black.

Shipping

Shipping costs are included in the reprint prices. Domestic orders are shipped via FedEx Ground service. Foreign orders are shipped via a proof of delivery air service.

Multiple Shipments

Orders can be shipped to more than one location. Please be aware that it will cost $32 for each additional location.

Delivery

Your order will be shipped within 2 weeks of the journal print date. Allow extra time for delivery.

Tax Due

Residents of Virginia, Maryland, Pennsylvania, and the District of Columbia are required to add the appropriate sales tax to each reprint order. For orders shipped to Canada, please add 7% Canadian GST unless exemption is claimed.

Ordering

Reprint order forms and purchase order or prepayment is required to process your order. Please reference journal name and reprint number or manuscript number on any correspondence. You may use the reverse side of this form as a proforma invoice. Please return your order form and prepayment to:

Cadmus Reprints
P.O. Box 751903
Charlotte, NC 28275-1903

Note: Do not send express packages to this location, PO Box.
FEIN #:541274108

Please direct all inquiries to:

Rose A. Baynard
800-407-9190 (toll free number)
410-819-3966 (direct number)
410-820-9765 (FAX number)
baynardr@cadmus.com (e-mail)

Reprint Order Forms and purchase order or prepayments must be received 72 hours after receipt of form.